JOURNAL OF MATERIALS SCIENCE **36** (2001) 2203–2212

Tensile properties of short fiber composites with fiber strength distribution

M. MAALEJ
Department of Civil Engineering, National University of Singapore, Singapore 119260
E-mail: cvemm@nus.edu.sg

The influence of fiber rupture, fiber pull-out and fiber tensile strength distribution on the post-cracking behavior of short-randomly-distributed fiber reinforced brittle-matrix composites has been analyzed using an approach based on the Weibull weakest-link statistics. The analysis led to the development of a predicting model for the composite bridging stress-crack opening displacement ($\sigma_c - \delta$) law—a fundamental material property necessary for the analysis of steady-state cracking in the composites. The proposed $\sigma_c - \delta$ relationship can be used to relate the composite tensile and fracture properties to the microstructural parameters. The model revealed the importance of fiber strength distribution as described by the Weibull weakest-link statistics in governing the post-cracking response of the composite. The proposed model was able to reproduce the results of an earlier model for a limiting case where fiber tensile rupture was accounted for assuming a deterministic fiber tensile rupture strength. Model-predicted post-peak $\sigma_c - \delta$ curve was also in close agreement with those obtained from uniaxial tensile tests of a Kevlar fiber reinforced cementitious composite where fiber tensile rupture was reported. The model provided physical insights as to the micro-mechanisms controlling the post-cracking response of short-fiber reinforced brittle-matrix composites where fibers have a tensile strength distribution described by the Weibull weakest-link statistics.

1. Introduction

The post-cracking behavior of short-fiber reinforced brittle-matrix composites can be predicted by the use of a composite bridging stress-crack opening displacement ($\sigma_c - \delta$) relationship. The $\sigma_c - \delta$ relationship describes the constitutive relationship between the traction (σ_c) acting across a matrix crack plane and the separation distance (δ) of the crack faces in a singly pre-cracked uniaxial tensile specimen loaded quasi-statically to complete failure [1]. The $\sigma_c - \delta$ curve consists of an ascending branch called the pre-peak $\sigma_c - \delta$ curve and a descending branch called the post-peak $\sigma_c - \delta$ curve (also referred to as the tension softening curve). The pre-peak $\sigma_c - \delta$ relationship is an important material property that governs the composite first cracking strength and the conditions for pseudo-strain hardening associated with multiple cracking in the composite [2].

An analytical model for the composite bridging stress-crack opening displacement relationship of short-randomly-distributed fiber reinforced brittle-matrix composites was initially proposed by Li [3] for the case of no fiber rupture. In a later study, Maalej *et al.* [4] extended this model to account for potential fiber tensile rupture. The extended model is referred to as the fiber pull-out and rupture model (FPRM). However, these analytical models have the limitation that fibers are assumed to exhibit a deterministic tensile rupture strength. A consequence of this assumption is that rupturing fibers must fail at the location of highest stress, which is at the matrix crack plane. Furthermore, in the absence of a fiber/matrix frictional effect called snubbing [5], fiber rupture is assumed to occur all-at-once when the crack opening displacement reaches a critical value at which the stress in the fiber is equal to the tensile rupture strength [4].

While ductile fibers such as steel fibers and polyethylene fibers can be assumed to have deterministic tensile rupture strengths, brittle fibers such as carbon fibers were reported to exhibit tensile strength distributions. Chi *et al.* [6] studied the tensile strength distribution of carbon fibers. Their study indicated that the tensile strength of carbon fibers follows a two-parameter Weibull distribution function. The Weibull's statistical theory [7, 8] is based on the "weakest link" concept where the strength of a material is assumed to be governed by the weakest strength of a large number of strengths.

Oh and Finnie [9] studied the statistical failure locations of a brittle body under various loading conditions. By adopting the Weibull weakest-link statistics and following the analysis of Oh and Finnie [9] and Matthews *et al.* [10], Thouless and Evans [11] proposed an analytical model which predicts the average fiber stress-displacement relationship in continuous-aligned fiber reinforced ceramics. In this paper, a

mathematical model for predicting the complete $\sigma_c - \delta$ relationship is derived for a brittle-matrix reinforced with short, randomly-distributed fibers having a tensile strength distribution satisfying the Weibull's weakest-link statistics.

2. Single-fiber stress-displacement relationship

Consider a single fiber bridging a plane crack as shown in Fig. 1. Following a shear-lag analysis, Li and Leung [2] developed a relationship between the debonding length y and the stress in the fiber σ_d:

$$\sigma_d = \frac{4\tau(1+\eta)}{d_f} y \tag{2}$$

$$y = \frac{d_f}{4\tau(1+\eta)} \sigma_d = \lambda \sigma_d \tag{3}$$

where

$$\eta = \frac{V_f E_f}{V_m E_m}$$

and

$$\lambda = \frac{d_f}{4\tau(1+\eta)}.$$

In their model, debonding was interpreted as the activation of a frictional bond stress τ between the fiber and the matrix. In addition, they derived a fiber stress-displacement relationship:

$$\sigma_d = \sqrt{\frac{4\tau(1+\eta)E_f\delta}{d_f}} = \frac{L_f}{2\lambda_e}\left(\frac{\hat{\delta}}{\hat{\delta}^*}\right)^{\frac{1}{2}} \quad \text{for} \quad 0 \le \delta \le \delta_0 \tag{4}$$

$$\sigma_p = \frac{4\tau(\ell + \delta_0 - \delta)}{d_f} \quad \text{for} \quad \delta_0 \le \delta \le \ell \tag{5}$$

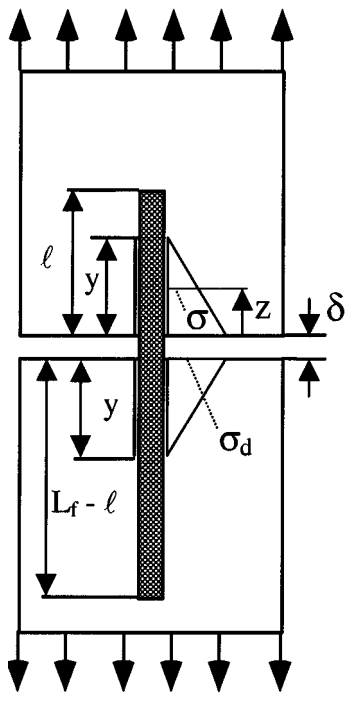

Figure 1 Single fiber bridging a plane crack.

where

$$\hat{\delta}^* = \frac{2\tau L_f}{(1+\eta)E_f d_f}, \quad \hat{\delta} = \frac{\delta}{(L_f/2)}$$

and

$$\delta_0 = \frac{4\tau\ell^2}{(1+\eta)E_f d_f}.$$

At the moment of complete debonding ($\delta = \delta_0$), the stress in the fiber is at its maximum value:

$$\sigma_p^{\max} = \sigma_d^{\max} = \frac{4\tau\ell}{d_f} = \frac{\ell}{\lambda_e} \tag{6}$$

where $\lambda_e = d_f/4\tau$. Within the debonding length y the bond stress τ is assumed constant. By neglecting the elastic bond stress, one can write the fiber axial stress as a function of location z within the debonding length:

$$\sigma(\sigma_d, z) = \sigma_d\left(1 - \frac{z}{y}\right) \tag{7}$$

3. Modeling fiber rupture

Based on weakest-link statistics, Thouless and Evans [11] derived a probability density function for fiber failure as a function of the peak stress σ_d and the distance from the crack plane z:

$$\Phi(\sigma_d, z) = \pi d_f \exp\left\{-2\int_0^y \pi d_f\left[\frac{\sigma(\sigma_d, z)}{S_0}\right]^m dz\right\} \times \frac{\partial}{\partial\sigma_d}\left[\frac{\sigma(\sigma_d, z)}{S_0}\right]^m \tag{8}$$

where $S_0 = \sigma_0 A_0^{1/m}$ is the scale parameter (or characteristic stress) and m is the Weibull modulus (or shape parameter). The parameters S_0 and m can be experimentally obtained by conducting single-fiber strength tests on specimens having unit surface area A_0 ($= \pi d_f L_0$). The stress σ_0 depends on the choice of the unit surface area of fiber A_0 in such a way that $S_0 = \sigma_0 A_0^{1/m}$ is constant. For infinitely large values of m the stress σ_0 may be interpreted as the deterministic tensile strength of the fiber. A lower value of m would indicate a greater variability in the fiber tensile strength. A typical value of Weibull modulus for carbon fibers is about 5 [6]. Using Equations 3 and 7 in Equation 8 we get:

$$\Phi(\sigma_d, z) = \frac{m(m+1)}{2\lambda S^{m+1}} \exp\left[-\left(\frac{\sigma_d}{S}\right)^{m+1}\right] \times \left(\sigma_d - \frac{z}{\lambda}\right)^{m-1} \tag{9}$$

where

$$S = \left[\frac{S_0^m(1+m)}{2\pi d_f \lambda}\right]^{\frac{1}{m+1}}$$

The failure probability of fibers having an embedment length ℓ is given by:

$$q_f(\ell) = 2\int_0^{\frac{\ell}{\lambda_e}} \int_0^{y=\lambda\sigma_d} \Phi(\sigma_d, z)\, dz\, d\sigma_d \qquad (10)$$

The factor 2 used in Equation 10 accounts for the fact that fibers could fail on either side of the crack, and therefore, both sides of the crack must be considered. Note that the maximum stress that the fibers will subjected to is equal to ℓ/λ_e (as per Equation 6). The survival probability of fibers having an embedment length ℓ is given by:

$$q_s(\ell) = 1 - q_f(\ell) = \exp\left[-\left(\frac{\ell}{\lambda_e S}\right)^{m+1}\right] \qquad (11)$$

Fig. 2 shows how the survival probability q_s depends on the fiber embedment length ℓ for different values of Weibull moduli m where the composite has the following microstructural properties: $V_f = 0.02$, $E_m = 13{,}000$ MPa, $E_f = 69{,}800$ MPa, $\tau = 4.5$ MPa, $d_f = 0.012$ mm, $L_f = 12.7$ mm, $A_0 = 0.48$ mm^2 and $\sigma_0 = 3310$ MPa. For low values of m, the figure indicates that fibers with short emdedment lengths have high survival probability while fibers with long embedment lengths have small survival probability. More specifically, when m is equal to 5, fibers with embedment length less than $\ell_{cs} = 1$ mm have a 100% survival probability while fibers with embdement length greater than $\ell_{cf} = 5$ mm have a 0% survival probability. As m increases, the gap between ℓ_{cs} and ℓ_{cf} gets smaller and both ℓ_{cs} and ℓ_{cf} approach a critical value $\ell_c = Sd_f/4\tau$. If m is increased while S_0 is kept constants, ℓ_c would approach the critical embedment length $L_c = \sigma_0 d_f/4\tau$ defined in the FPRM [4] where σ_0 is interpreted as the deterministic tensile strength of the fiber.

The failure probability of fibers having an embedment length ℓ at a crack opening displacement $\delta \le \delta_0$ is given by:

$$q_f(\delta) = 2\int_0^{\frac{L_f}{2\lambda_e}\left(\frac{\hat{\delta}}{\hat{\delta}^*}\right)^{1/2}} \int_0^{y=\lambda\sigma_d} \Phi(\sigma_d, z)\, dz\, d\sigma_d \qquad (12)$$

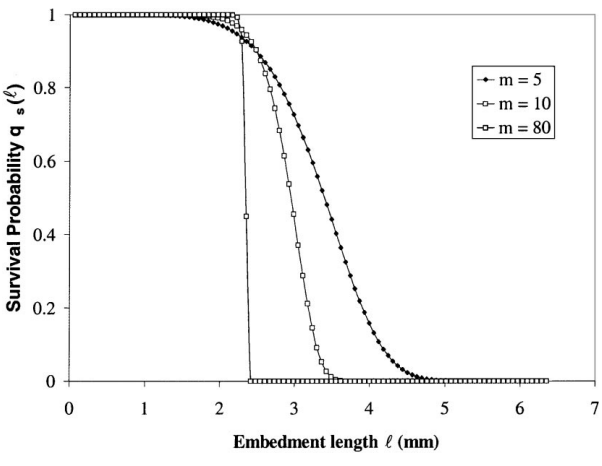

Figure 2 Effect of fiber embedment length on the survival probability.

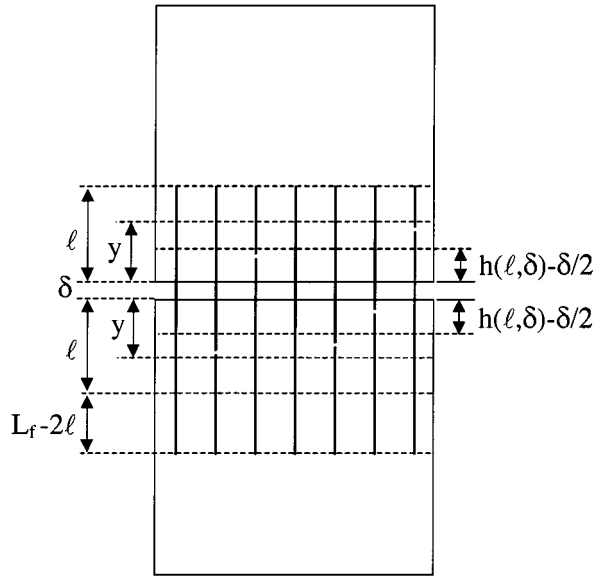

Figure 3 Mean failure position for rupturing fibers with embedment length ℓ when the COD is δ.

The corresponding survival probability $q_s(\delta)$is then:

$$q_s(\delta) = 1 - q_f(\delta) = \exp\left[-\left(\frac{L_f}{2\lambda_e S}\left(\frac{\hat{\delta}}{\hat{\delta}^*}\right)^{1/2}\right)^{m+1}\right] \qquad (13)$$

The average failure position for rupturing fibers with embedment length ℓ at a crack opening displacement $\delta \le \delta_0$ is given by (see Fig. 3):

$$h(\ell, \delta) = \frac{2\int_0^{\frac{L_f}{2\lambda_e}\left(\frac{\hat{\delta}}{\hat{\delta}^*}\right)^{\frac{1}{2}}} \int_0^{y=\lambda\sigma_d} z\Phi(\sigma_d, z)\, dz\, d\sigma_d}{2\int_0^{\frac{\ell}{\lambda_e}} \int_0^{y=\lambda\sigma_d} \Phi(\sigma_d, z)\, dz\, d\sigma_d}$$
$$= \frac{\lambda S}{(m+1)q_f(\ell)}\Gamma\left[\frac{m+2}{m+1}, 0, \left(\frac{L_f}{2\lambda_e S}\left(\frac{\hat{\delta}}{\hat{\delta}^*}\right)^{\frac{1}{2}}\right)^{m+1}\right] \qquad (14)$$

where $\Gamma[a, x_1, x_2]$ is the generalized incomplete gamma function defined by:

$$\Gamma[a, x_1, x_2] = \int_{x_1}^{x_2} t^{a-1}e^{-t}\, dt \qquad (15)$$

The average failure position when all fibers (with embedment length ℓ) have failed ($\delta \ge \delta_0$):

$$h(\ell) = \frac{\lambda S}{(m+1)q_f(\ell)}\Gamma\left[\frac{m+2}{m+1}, 0, \left(\frac{\ell}{\lambda_e S}\right)^{m+1}\right] \qquad (16)$$

The average tensile strength of rupturing fibers with embedment length ℓ taking into account the fiber stress

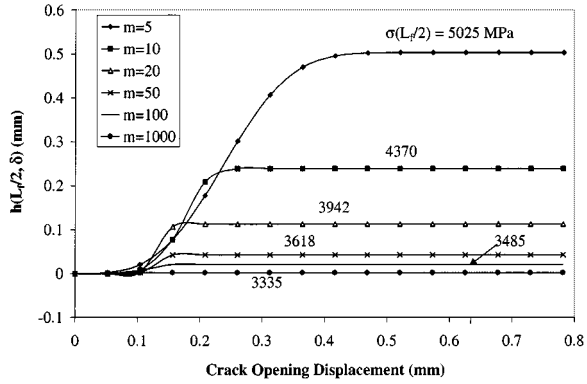

Figure 4 Effect of Weibull modulus on the mean location of fiber rupture for fibers with embedment length $\ell = L_f/2$.

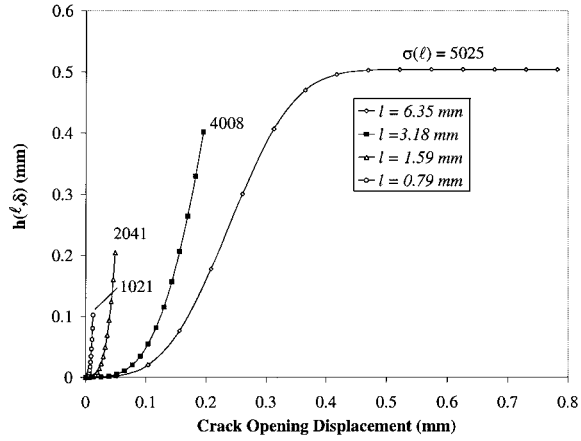

Figure 5 Variation of mean failure position as function of δ for different fiber embedment lengths ℓ.

distribution is given by:

$$\sigma(\ell) = \frac{2\int_0^{\frac{\ell}{\lambda_e}} \int_0^{y=\lambda\sigma_d} \sigma_d \Phi(\sigma_d, z)\, dz\, d\sigma_d}{2\int_0^{\frac{\ell}{\lambda_e}} \int_0^{y=\lambda\sigma_d} \Phi(\sigma_d, z)\, dz\, d\sigma_d} = \frac{S}{q_f(\ell)}$$
$$\times \Gamma\left[\frac{m+2}{m+1}, 0, \left(\frac{\ell}{\lambda_e S}\right)^{m+1}\right] = \frac{m+1}{\lambda} h(\ell) \qquad (17)$$

Fig. 4 shows the effect of Weibull modulus m on the variation of average fiber failure position $h(L_f/2, \delta)$ as function of crack opening displacement for a composite with the same microstructural properties as that shown in Fig. 2. As indicated, the average failure position increases as function of COD. The maximum crack opening displacement shown corresponds to the COD δ^* (0.78 mm) at which complete debonding of the fibers with the longest embedment length ($\ell = L_f/2$) takes place. After this stage, no more fiber rupture will take place. It is apparent from Fig. 4 that fiber rupture takes place in a more progressive manner when m is small. The figure also indicates that as the Weibull modulus increases the mean failure position gets smaller. From the behavioral trends shown in Fig. 4, it appears that in the limit when m approaches infinity, $h(L_f/2, \delta)$ approaches zero for any value of δ. This would be the case of fibers with a deterministic tensile rupture strength. For each value of m, the figure also shows the average tensile strength for all fibers with embedment length equal to $L_f/2$. As m gets larger, the average tensile strength approaches σ_0 where $S_0 = \sigma_0 A_0^{1/m}$ is the scale parameter.

Fig. 5 shows the variation of mean fiber failure position as function of COD for different fiber embedment lengths ($m = 5$ in this case). For each curve, the last data point shown corresponds to the condition where the fiber has completely debonded ($\delta = \delta_0$). As indicated, the maximum $h(\ell, \delta)$ is always a fraction of the embedment length ℓ and decreases with decreasing values of ℓ. Also shown in that plot is the average tensile strength of all rupturing fibers with embedment length ℓ for each value of ℓ. The figure shows that the average tensile strength decreases with decreasing values of ℓ. This is consistent with what one would expect given that if a fiber with short emdedment length ℓ has to fail, failure would have to be at a low value of stress. This is the case because the maximum stress that can develop in a fiber is proportional to the fiber embedment length (see Equation 6).

4. Composite bridging stress-crack opening displacement ($\sigma_c - \delta$) law

Li *et al.* [12] showed that the $\sigma_c - \delta$ curve can be predicted by summing the contributions of the individual fibers intersecting the matrix crack plane, according to the following relationship:

$$\sigma_c = V_f \int_0^{\frac{\pi}{2}} \int_0^{(L_f/2)\cos\theta} \sigma_b(\delta, \theta, w) p(w) p(\theta)\, dw\, d\theta \qquad (18)$$

where $\sigma_b(\delta, \theta, w)$ is the fiber bridging stress and $p(w)$ and $p(\theta)$ are probability density functions of the orientation angle and centroidal distance of fibers from the matrix crack plane. For a uniform random distribution $p(w)$ and $p(\theta)$ are defined as follows:

$$p(w) = \frac{2}{L_f} \quad \text{for} \quad 0 \le w \le \frac{L_f}{2}\cos(\theta) \qquad (19)$$

$$p(\theta) = \sin\theta \quad \text{for} \quad 0 \le \theta \le \frac{\pi}{2} \qquad (20)$$

The inclination of the fiber with respect to the matrix crack plane (see Fig. 6) could result in an additional

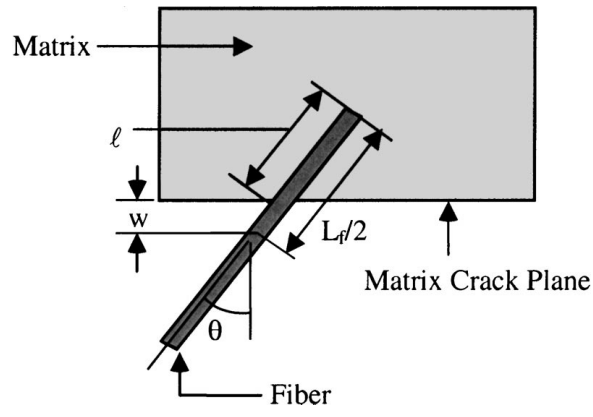

Figure 6 Definition of fiber embedment length ℓ, centroidal location w and inclination angle θ.

frictional effect called snubbing [5]. When present, the snubbing effect results in an amplification of the stress in the fiber at the point where it exits from the matrix. This effect has been experimentally observed in nylon and polypropylene fiber reinforced mortar [5]. The inclusion of the snubbing effect in the present formulation will render the solution analytically unmanageable. To simplify the analysis, the snubbing effect is therefore assumed to be negligible. Accordingly, the fiber bridging stress $\sigma_b(\delta, \theta, w)$ will be given by:

$$\sigma_b(\delta, \theta, w) = \begin{cases} \sigma_d = \dfrac{L_f}{2\lambda_e}\left(\dfrac{\hat{\delta}}{\hat{\delta}^*}\right)^{\frac{1}{2}} & \text{for} \quad 0 \le \delta \le \delta_0 \quad (21a) \\ \sigma_p = \dfrac{4\tau(\ell + \delta_0 - \delta)}{d_f} & \text{for} \quad \delta_0 \le \delta \le \ell \\ \quad = \dfrac{L_f}{2\lambda_e}\left(x - \hat{\delta}^* x^2 - \hat{\delta}\right) & (21b) \end{cases}$$

where $x = \ell/(L_f/2)$. With the change of variable

$$x = \frac{2}{L_f}\ell = \frac{2}{L_f}\left(\frac{L_f}{2} - \frac{w}{\cos\theta}\right)$$

Equation 18 becomes:

$$\sigma_c = \frac{V_f}{2}\int_0^{\frac{\pi}{2}}\int_0^1 \sigma_b(\delta, \theta, x)\sin(2\theta)\, dx\, d\theta \quad (22)$$

$$\sigma_c = \frac{V_f}{2}\int_0^1 \sigma_b(\delta, x)\, dx \quad (23)$$

To derive the governing relationship for the complete $\sigma_c - \delta$ curve, it would be convenient to separately consider two distinct branches of this curve—The debonding $\sigma_c - \delta$ branch and the pull-out $\sigma_c - \delta$ branch.

4.1. Debonding $\sigma_c - \delta$ branch

The debonding $\sigma_c - \delta$ branch consists of the contributions of two different fiber groups. In the first group, fibers completely debond and then pull-out. These are the surviving fibers. Fibers with the longest embedment length ($\ell = L_f/2$) will completely debond when $\delta = \delta^*$. Therefore, the debonding $\sigma_c - \delta$ branch corresponds to the portion of the $\sigma_c - \delta$ curve for which $\delta \le \delta^*$. At each value of δ, a fraction of the fibers are in a debonding mode, while the others (with short embedment lengths) are either in a pull-out mode or have completely pulled-out of the matrix and no longer contribute to the composite bridging stress. This is explicitly accounted for by proper selection of the integration points in Equation 23 as shown in Appendix A. The contribution of the surviving fibers is computed by multiplying the fiber bridging stress by $q_s(\ell)$.

The second group of fibers consists of those fibers which rupture sometime during the debonding process. The contribution of these fibers is computed by multiplying the fiber bridging stress by $q_f(\ell)$. Within this group of fibers, at each value of COD δ, some fibers are in a debonding mode while others are in a pull-out mode. The contribution of the first subgroup is computed by multiplying the fiber bridging stress by $q_s(\delta)$. The contribution of the second subgroup is computed by multiplying the fiber bridging stress by $q_f(\delta)$. Note that the fiber bridging stress for this subgroup of fibers depends on the mean fiber failure position $h(\ell, \delta)$ as shown in the appendix. Therefore, rupturing fibers would still contribute to the composite bridging stress through frictional fiber pull-out. However, this contribution is quite small compared to that of the surviving fibers. This is unlike the case of continuous-aligned fiber reinforced composites where rupturing fibers are the only contributors to the frictional fiber pull-out portion of the $\sigma_c - \delta$ curve. The complete derivation of the debonding $\sigma_c - \delta$ branch is given in Appendix A. After dropping the negligible contribution of rupturing fiber to frictional fiber pull-out and summing all other contributions, the following expression of the $\sigma_c - \delta$ relationship is obtained:

$$\begin{aligned} \hat{\sigma}_c = {} & \left(\frac{\hat{\delta}}{\hat{\delta}^*}\right)^{1/2}\Gamma\left[a, t^*, t_0(\hat{\delta})\right] + \hat{\delta}^*[x^*]^2 \\ & \times \Gamma\left[3a, t_0(\hat{\delta}), t_1(\hat{\delta})\right] + x^*\Gamma\left[2a, t_0(\hat{\delta}), t_1(\hat{\delta})\right] \\ & - \hat{\delta}\Gamma[a, t_0(\hat{\delta}), t_1(\hat{\delta})] + q_s(\hat{\delta})\left(\frac{\hat{\delta}}{\hat{\delta}^*}\right)^{1/2} \\ & \times \left\{\frac{m+1}{x^*}\left[1 - \left(\frac{\hat{\delta}}{\hat{\delta}^*}\right)^{1/2}\right] - \Gamma\left[a, t^*, t_0(\hat{\delta})\right]\right\} \\ & \text{for} \qquad \hat{\delta} \le \hat{\delta}^* \end{aligned} \quad (24)$$

where

$$\hat{\sigma}_c = \frac{\sigma_c}{g\left(\dfrac{S}{m+1}\right)\left(\dfrac{V_f}{2}\right)}, \quad a = \frac{1}{m+1},$$

$$x^* = \frac{\lambda_e S}{L_f/2}, \quad t^* = \left(\frac{1}{x^*}\right)^{m+1},$$

$$t_0(\hat{\delta}) = \left(\frac{1}{x^*}\left(\frac{\hat{\delta}}{\hat{\delta}^*}\right)^{1/2}\right)^{m+1}, \quad t_1(\hat{\delta}) = \left(\frac{\hat{\delta}}{x^*}\right)^{m+1}$$

and

$$x_0 = \left(\frac{\hat{\delta}}{\hat{\delta}^*}\right)^{\frac{1}{2}}$$

4.2. Pull-out $\sigma_c - \delta$ branch

The Pull-out $\sigma_c - \delta$ branch corresponds to the portion of the $\sigma_c - \delta$ curve for which $\delta \ge \delta^*$. Two different groups contribute to this branch. The first group consists of those fibers that have survived and are in a pull-out mode. The second group corresponds to those fibers that have failed during debonding and are also in a pull-out mode. The contribution of the fibers from the second group was found to be very negligible compared to the one from the first group. After dropping the negligible

contribution of the second group of fibers, the post-peak $\sigma_c - \delta$ relationship would be given by:

$$\hat{\sigma}_c = \hat{\delta}^*[x^*]^2\Gamma\left[3a, t^*, t_1(\hat{\delta})\right] + x^*\Gamma\left[2a, t^*, t_1(\hat{\delta})\right] - \hat{\delta}\Gamma\left[a, t^*, t_1(\hat{\delta})\right] \quad (25)$$

5. Discussion of the $\sigma_c - \delta$ curve and experimental verification

Fig. 7 shows the complete $\sigma_c - \delta$ curve for a composite with the same microstructural properties as the one presented in Fig. 2. For this composite δ^* is equal to 0.781 mm and the composite bridging stress becomes equal to zero when δ is equal to approximately 4 mm. The ultimate composite bridging stress σ_{cu} occurs at a COD δ_u equal to 0.135 mm. In what follows, the portion of the $\sigma_c - \delta$ curve for which $\delta \leq \delta_u$ will be referred to as the pre-peak $\sigma_c - \delta$ curve and that for which $\delta > \delta_u$ will be referred to as the post-peak $\sigma_c - \delta$ curve.

Fig. 8 shows a comparison between model-predicted and experimentally-measured post-peak $\sigma_c - \delta$ curves for a cementitious composite with 2% by volume of Kevlar fiber reinforcement. The original data was reported by Maalej *et al.* [4]. Post-test examination of the fracture surface revealed that a significant proportion of the reinforcing fibers have ruptured in the composite. The microstructural parameters used in the predicting model were as follows: $V_f = 0.02$, $E_m = 13,000$ MPa, $E_f = 69,800$ MPa, $\tau = 4.5$ MPa, $d_f = 0.012$ mm, $L_f = 12.7$ mm, $m = 100$ and $S_0 = \sigma_0 A_0^{1/m}$ (where $A_0 = 1$ mm^2 and $\sigma_0 = 2700$ MPa). Except for m and S_0, all values of microstructural parameters are actual. The interfacial bond strength has been independently measured by Wang [13]. In the absence of independently-determined m and S_0 for Kevlar fibers, the assumed values seem to represent well the experimental data. The relatively high value of m used implies that Kevlar fibers are assumed to have a narrow fiber strength distribution.

Note that in most fiber reinforced cementitious composites the complete pre-peak $\sigma_c - \delta$ curve is very difficult to measure. Part of the difficulty is that the microcrack opening is very small at this fiber bridging stage, and in ordinary fiber reinforced cementitious composites, this portion is completely masked by the matrix strength. This means that as soon as the matrix cracks, the load has already exceeded the maximum bridging strength of the fibers, and only the post-peak portion is revealed in the experiment. This condition is schematically illustrated in Fig. 9. The figure shows that the crack has not completely propagated through the specimen, but the crack opening displacement at the midpoint of the crack δ_m has already exceeded the COD δ_u corresponding to the maxima of the composite bridging stress σ_{cu}. By the time the crack reaches both edges of the specimen, the composite bridging stress transferred across the matrix crack would be on the post-peak

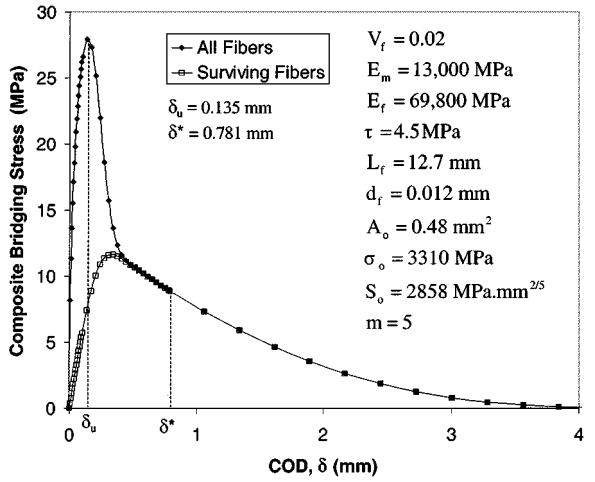

Figure 7 Complete $\sigma_c - \delta$ curve showing the contribution of surviving fibers.

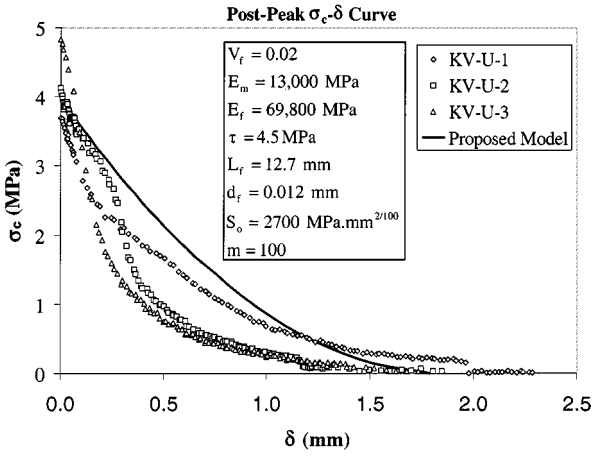

Figure 8 Comparison between model-predicted and experimentally-measured post-peak $\sigma_c - \delta$ curves.

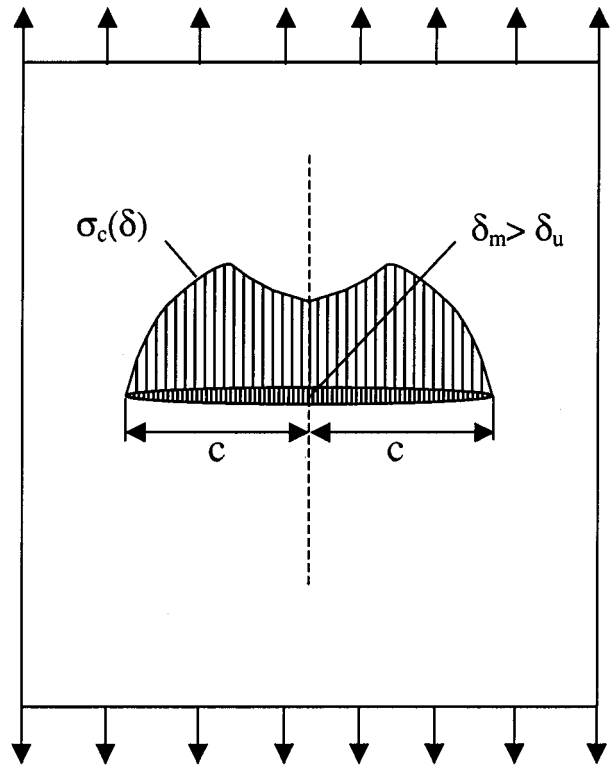

Figure 9 Propagating matrix crack bridged by fibers. The figure illustrates a condition where the pre-peak $\sigma_c - \delta$ curve can-not be obtained from a uniaxial tension test.

$\sigma_c - \delta$ curve. This is believed to be the reason why the pre-peak $\sigma_c - \delta$ curve was not captured for the 2% Kevlar fiber composite.

6. Parametric study

Fig. 10 shows the effect of Weibull modulus m on the $\sigma_c - \delta$ curve. As indicated, composites with lower values of m have higher ultimate composite bridging stresses σ_{cu}. In this case, fiber rupture occurs in a more progressive manner—allowing a significant proportion of fibers to transfer higher stresses across the matrix crack. As the Weibull modulus increases, σ_{cu} decreases but the rate of stress loss from the peak increases. For large values of m (i.e. $m > 100$), the present model predicted a $\sigma_c - \delta$ curve that is close agreement with that obtained from the FPRM model (which assumes that fibers have a deterministic tensile rupture strength). In this case, the curve shows a sudden drop in stress from the peak due to fiber rupture. As discussed earlier, when a deterministic tensile rupture strength is assumed, all fibers with large embedment lengths ($\ell \geq L_c = \sigma_{fu} d_f / 4\tau$) fail when the COD reaches a critical value equal to δ_c. In this case, the post-peak portion of the $\sigma_c - \delta$ curve is due to the contribution of the surviving fibers (fibers with embedment length $\ell < L_c$).

Fig. 11 shows a series of $\sigma_c - \delta$ curves for the same composite with different lengths of fibers. As the figure shows, composites with longer fiber lengths have higher composite peak stresses. This is the case because

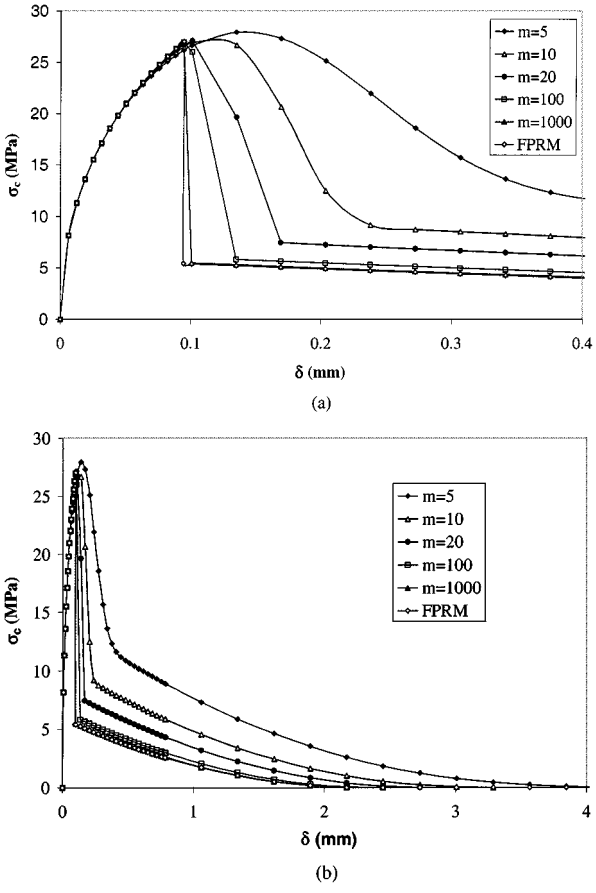

Figure 10 Effect of Weibull modulus on $\sigma_c - \delta$ curve. (a) Pre-peak $\sigma_c - \delta$ curve. (b) Complete $\sigma_c - \delta$ curve.

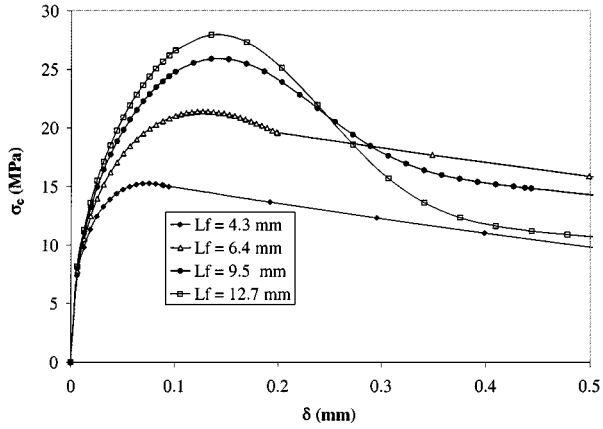

Figure 11 Effect of fiber length on $\sigma_c - \delta$ curve.

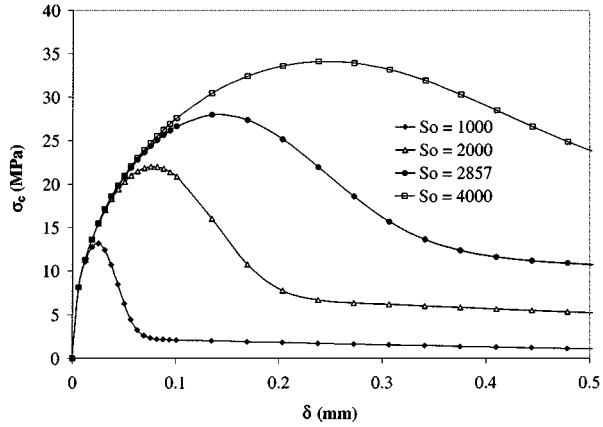

Figure 12 Effect of scale parameter (characteristic stress) on $\sigma_c - \delta$ curve.

at each value of δ, longer fibers provide more effective stress transfer across the matrix crack. As larger proportions of fibers carry higher stresses, larger proportions of fibers fail as well. This is why there is a sharper drop in the bridging stress from the peak for composites with longer fiber lengths. If one defines the composite bridging fracture energy G_c as the area under the $\sigma_c - \delta$ curve, one can conclude that below a critical value of L_f, an increase in the length of the fiber is associated with an increase in both σ_{cu} and G_c. However, above the same critical value, an increase in L_f is associated with an increase in σ_{cu} but a decrease in G_c.

Fig. 12 shows the effect of scale parameter S_0 on the $\sigma_c - \delta$ curve for the same composite. As indicated, a composite with a higher scale parameter S_0 has also higher composite bridging strength and fracture energy. At the micro-structural level, an increase in S_0 results in delaying the occurrence of fiber rupture as well as reducing the proportions of rupturing fibers. The former results in increasing the composite bridging strength while the latter results in increasing the composite bridging fracture energy.

Figs 13 and 14 show the effects of interfacial bond strength and fiber diameter on the $\sigma_c - \delta$ curve, respectively. These figures indicate that both parameters influence the $\sigma_c - \delta$ curve in the same manner as does the length of the fiber. Both figures indicate the presence of a critical interfacial bond strength (assuming that all other parameters are held constant) and a critical fiber

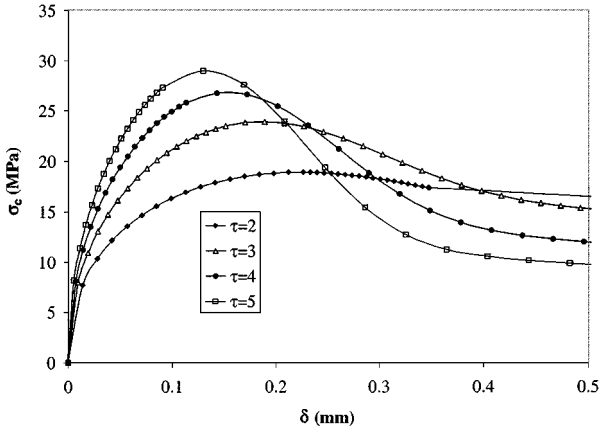

Figure 13 Effect of interfacial bond strength on $\sigma_c - \delta$ curve.

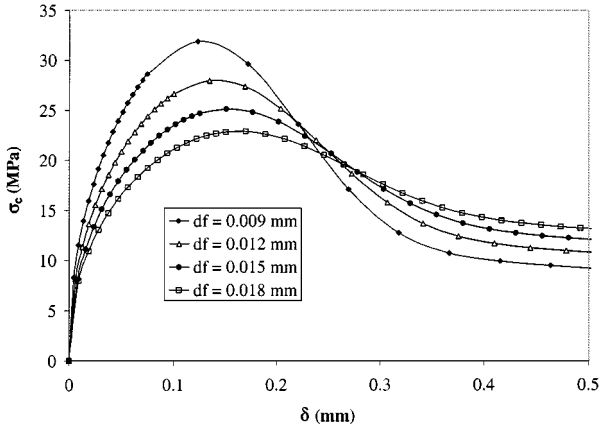

Figure 14 Effect fiber diameter on $\sigma_c - \delta$ curve.

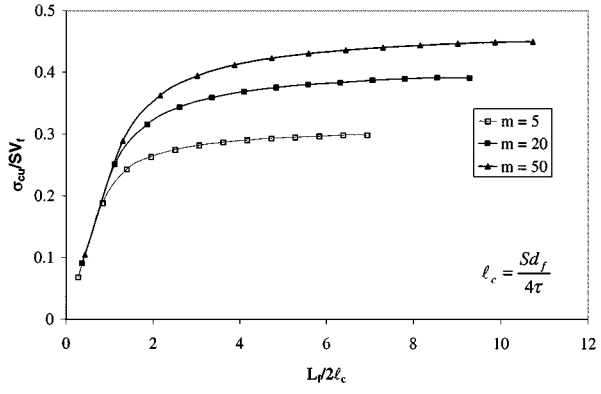

Figure 15 Effect fiber length on the composite bridging strength.

diameter for the composite. Up to the critical value of interfacial bond strength, an increase in τ results in an increase in both σ_{cu} and G_c. Thereafter, an increase in τ is associated with an increase in σ_{cu} and a decrease in G_c. For fiber diameter, above the critical value, a reduction in d_f increases both σ_{cu} and G_c. Below this critical value, however, a reduction in fiber diameter positively affects σ_{cu} while negatively affecting G_c.

Fig. 15 shows the variation of normalized composite bridging strength as function of normalized fiber length. For a given value of Weibull modulus m, the normalizing parameter S (which has units of stress) can be thought of as the average tensile strength of the fiber. As indicated, an increase in the length of the fiber is associated with an increase in the composite bridging strength. However, the rate of strength increase starts to diminish when the normalized fiber length is greater than 2. The observed trend suggests that this rate eventually becomes equal to zero. If S is thought of as the average tensile strength of the fiber, one can conclude that as the normalized fiber length approaches 2, the average tensile stress in the fiber starts to approach S. Once S is reached, no further increase in the average tensile stress of the fiber is expected. For each value of m, the normalized composite bridging strength approaches a limiting value when the length of the fiber becomes very large. As m gets larger, this limiting value appears to approach 0.5. This result is consistent with the classical concept that when fibers are infinitely long and randomly oriented in three dimensions, the number of fibers crossing a planar matrix crack is equal to half the number if all fibers were oriented in a direction perpendicular to the matrix crack [14]. In either case, the post cracking strength would be equal to the number of fibers times the maximum load transferred by each fiber. For infinitely long fibers, randomly oriented in three dimensions in a brittle matrix, the composite post-cracking strength would be equal to 0.5 $V_f\sigma_{fu}$ where σ_{fu} is the tensile strength of the fiber.

7. Conclusions

The structural performance of a fiber reinforced brittle matrix composite can be related to the material post-cracking behavior ($\sigma_c - \delta$ law) as well as the component size and geometry. For this reason it is important to be able to determine how the $\sigma_c - \delta$ law can be influenced by tailoring the microstructural parameters. The preceding discussion suggests that the Weibull modulus and characteristic stress have a significant effect on the composite $\sigma_c - \delta$ law. The presence of a fiber strength distribution induces a progressive fiber rupture mechanism which seemed to positively affect both the pre-peak and the post-peak $\sigma_c - \delta$ curves. The former was found to influence the conditions for steady-state cracking while the latter was found to influence the mechanism of slow crack propagation. In addition to the two parameters of the Weibull distribution, other parameters such as the length and diameter of the fiber as well as the interfacial bond strength would also influence the $\sigma_c - \delta$ curve. These parameters influence the state of stress in the fibers as well as the fiber/matrix stress transfer mechanism. The proposed model points to the existence of an optimum value for each one these parameters (assuming all others are held constant), thereby offering a range of possibilities on how the composite properties can be optimized.

Appendix A. Derivation of the $\sigma_c - \delta$ relationship

A.1. Debonding $\sigma_c - \delta$ branch

The debonding $\sigma_c - \delta$ branch consists of the contributions of two different groups of fibers. In the first group,

fibers completely debond and then pull-out, while in the second group fibers rupture during debonding. Thus

$$\sigma_c(\delta) = \sigma_{cs} + \sigma_{cf} = (\sigma_{csd} + \sigma_{csp}) + (\sigma_{cfd} + \sigma_{cfp}) \quad \delta \le \delta^* \quad \text{(A1)}$$

where

σ_{csd} = Contribution of surviving fibers to σ_c during debonding.
σ_{csp} = Contribution of surviving fibers to σ_c during pull-out.
σ_{cfd} = Contribution of failing fibers to σ_c during debonding.
σ_{cfp} = Contribution of failed fibers to σ_c during pull-out.

A.1.1. Surviving fibers

During debonding we should have:

$$\delta \le \delta_0 \Rightarrow x \ge x_0$$

where

$$x_0 = \left(\frac{\hat{\delta}}{\hat{\delta}^*}\right)^{\frac{1}{2}}.$$

Thus:

$$\sigma_{csd} = \frac{V_f}{2}\int_{x_0}^{1} q_s(x)\sigma_d\, dx \quad \text{(A2)}$$

where

$$q_s(x) = \exp\left[-\left(\frac{x}{x^*}\right)^{m+1}\right], \quad x^* = \frac{\lambda_e S}{(L_f/2)}$$

and

$$\sigma_d = \frac{S}{x^*}\left(\frac{\hat{\delta}}{\hat{\delta}^*}\right)^{\frac{1}{2}}$$

Evaluation of Equation A2 gives:

$$\hat{\sigma}_{csd} = \left(\frac{\hat{\delta}}{\hat{\delta}^*}\right)^{1/2}\Gamma\left[a, t^*, t_0(\hat{\delta})\right] \quad \text{(A3)}$$

where

$$\hat{\sigma}_{csd} = \frac{\sigma_{csd}}{\left(\frac{S}{m+1}\right)\left(\frac{V_f}{2}\right)}, \quad t^* = \left(\frac{1}{x^*}\right)^{m+1}$$

and

$$t_0(\hat{\delta}) = \left(\frac{1}{x^*}\left(\frac{\hat{\delta}}{\hat{\delta}^*}\right)^{1/2}\right)^{m+1}$$

During pull-out we should have: $\delta \le \ell \Rightarrow x \ge x_1$ where $x_1 = \hat{\delta}$, and $x \le x_0$. Thus

$$\sigma_{csp} = \frac{V_f}{2}\int_{x_1}^{x_0} q_s(x)\sigma_p\, dx \quad \text{(A4)}$$

$$\hat{\sigma}_{csp} = \hat{\delta}^*[x^*]^2\Gamma[3a, t_0(\hat{\delta}), t_1(\hat{\delta})] + x^* \times \Gamma[2a, t_0(\hat{\delta}), t_1(\hat{\delta})] - \hat{\delta}\Gamma[a, t_0(\hat{\delta}), t_1(\hat{\delta})] \quad \text{(A5)}$$

where

$$\sigma_p = \frac{S}{x^*}(x + \hat{\delta}^* x^2 - \hat{\delta})$$

A.1.2. Failing fibers

During debonding, the contribution of the failing fibers to σ_c is given by:

$$\sigma_{cfd} = \frac{V_f}{2}\int_{x_0}^{1} q_f(x)q_s(\delta)\sigma_d\, dx \quad \text{(A6)}$$

$$\hat{\sigma}_{cfd} = q_s(\hat{\delta})\left(\frac{\hat{\delta}}{\hat{\delta}^*}\right)^{1/2}\left\{\frac{m+1}{x^*}\left[1 - \left(\frac{\hat{\delta}}{\hat{\delta}^*}\right)^{1/2}\right] - \Gamma\left[a, t^*, t_0(\hat{\delta})\right]\right\} \quad \text{(A7)}$$

Note that $q_s(\delta)$ is used in Equation A6 to account for the contributions of only those fibers which did not fail yet at the COD δ.

For each value of $\delta \le \delta^*$, rupturing fibers with embedment length ℓ will have a mean fiber failure position equal to $h(\ell, \delta)$. The contribution of the failing fibers to σ_c during the sliding stage is valid for $\delta \le \delta_0$ (or $x \ge x_0$). Therefore, this contribution can be computed from the following equation:

$$\sigma_{cfp} = \frac{V_f}{2}\int_{x_0}^{1} q_f(x)q_f(\hat{\delta})\frac{S}{x^*}[\hat{h}(x, \hat{\delta}) - \hat{\delta}/2]\, dx \quad \text{(A8)}$$

$$\sigma_{cfp} = \int_{x_0}^{1} q_f(x)\frac{m+1}{x^*}q_f(\hat{\delta})[\hat{h}(x, \hat{\delta}) - \hat{\delta}/2]\, dx \quad \text{(A9)}$$

For each value of $\delta \le \delta^*$, numerical integration of Equation A9 is necessary to compute $\sigma_{cfp}(\delta)$.

A.2. Pull-out $\sigma_c - \delta$ branch

Two different groups contribute to the pull-out $\sigma_c - \delta$ branch. The first group consists of those fibers that have survived and are in a stage of pull-out. The second group corresponds to those fibers that have failed during debonding and are in a pull-out mode. Thus:

$$\sigma_c(\delta) = \sigma_{cs} + \sigma_{cf} \quad \delta \ge \delta^* \quad \text{(A10)}$$

where

σ_{cs} = Contribution of surviving fibers to σ_c during pull-out.
σ_{cf} = Contribution of failed fibers to σ_c during pull-out.

A.2.1. Surviving fibers

The contribution of the surviving fibers to σ_c is given by the following equation:

$$\sigma_{cs} = \frac{V_f}{2}\int_{x_1}^{1} q_s(x)\sigma_p\, dx \tag{A11}$$

$$\hat{\sigma}_{cs} = \hat{\delta}^*[x^*]^2\Gamma\left[3a, t^*, t_1(\hat{\delta})\right] + x^*\Gamma\left[2a, t^*, t_1(\hat{\delta})\right] - \hat{\delta}\Gamma\left[a, t^*, t_1(\hat{\delta})\right] \tag{A12}$$

A.2.2. Failed fibers

The contribution of the failed fibers to σ_c is given by the following equation

$$\sigma_{cf} = \frac{V_f}{2}\int_{x_2}^{1} q_f(x)\frac{S}{x^*}\left[\hat{h}(x) + \frac{\hat{\delta}^*}{2}x^2 - \hat{\delta}\right] dx \tag{A13}$$

$$\hat{\sigma}_{cf} = \int_{x_2}^{1} q_f(x)\frac{m+1}{x^*}\left[\hat{h}(x) + \frac{\hat{\delta}^*}{2}x^2 - \hat{\delta}\right] dx \tag{A14}$$

where

$$\hat{h}(x_2) + \frac{\hat{\delta}^*}{2}x_2^2 - \hat{\delta} = 0 \tag{A15}$$

To obtain $\sigma_{cf}(\delta)$ for each value of $\delta \geq \delta^*$, Equation A15 would have to be solved for x_2 and the integral in Equation A15 would have to be evaluated using numerical integration. By using x_2 as a lower limit in above integral, only those fibers with large values of $h(\ell)$ are counted as contributing fibers.

References

1. V. C. LI, C. M. CHAN and C. K. Y. LEUNG, *Cement and Concrete Research* **17** (1987) 441.
2. V. C. LI and C. K. Y. LEUNG, *ASCE J. of Engineering Mechanics* **118** (1992) 2246.
3. V. C. LI, *ASCE J. of Materials in Civil Engineering* **4** (1992) 41.
4. M. MAALEJ, V. C. LI and T. HASHIDA, *ASCE Journal of Engineering Mechanics* **121** (1995) 903.
5. V. C. LI, Y. WANG and S. BACKER, *J. Composites* **21** (1990) 132.
6. Z. CHI, T .W. CHOU and G. SHEN, *J. Mater. Sci.* **19** (1984) 3319.
7. W. WEIBULL, *Royal Swedish Academy Eng. Sci. Pro.* **151** (1939) 1.
8. *Idem., J. Applied Mech.* **18** (1951) 293.
9. H. L. OH and I. FINNIE, *International Journal of Fracture Mechanics* **6** (1970) 287.
10. J. R. MATTHEWS, F. A. McCLINTOCK and W. J. SHACK, *J. Amer. Ceram. Soc.* **59** (1976) 304.
11. M. D. THOULESS and A. G. EVANS, *Acta Metall.* **36** (1988) 517.
12. V. C. LI, Y. WANG and S. BACKER, *J. Mech. Phys. Solids* **39** (1991) 607.
13. Y. WANG, PhD thesis, Massachusetts Institute of Technology, Cambridge, Massachusetts, 1989.
14. J. AVESTON and A. KELLY, *J. Mater. Sci.* **8** (1973) 352.

Received 8 May
and accepted 27 October 2000